The giant plasticity of a quantum crystal - Supplemental Material

Ariel Haziot[1], Xavier Rojas[1], Andrew D. Fefferman[1], John R. Beamish[1,2], and Sébastien Balibar[1]

1- Laboratoire de Physique Statistique de lEcole Normale Suprieure,
associ au CNRS et aux Universits P.M. Curie and D. Diderot,
24 rue Lhomond, 75231 Paris Cedex 05, France.
2 - Departement of Physics, University of Alberta, Edmonton, Alberta Canada T6G 2G7

THE EXPERIMENTAL CELL AND THE TRANSDUCER CALIBRATION

Our experimental cell is a 5 cm^3 hexagonal hole in a 15 mm thick copper plate, which is closed on its back and front faces by glass windows sealed with Indium rings (see Figure 1) and stainless steel clamps. It is filled with ^{4}He through a thin Cu-Ni capillary (the "fill line" whose inner diameter is 0.4 mm). It stands at least 62 bar inner pressure. Inside this cell, we have glued two piezo-electric transducers [11] in order to shear crystals that are grown in the gap between them. The thickness of this gap was $d = 1.2$ mm in a first cell used for crystals from X1 to X6 and $d = 0.7$ mm in the second cell shown on Figure 1, where the transducers are glued on their whole surface area in order to avoid any possible
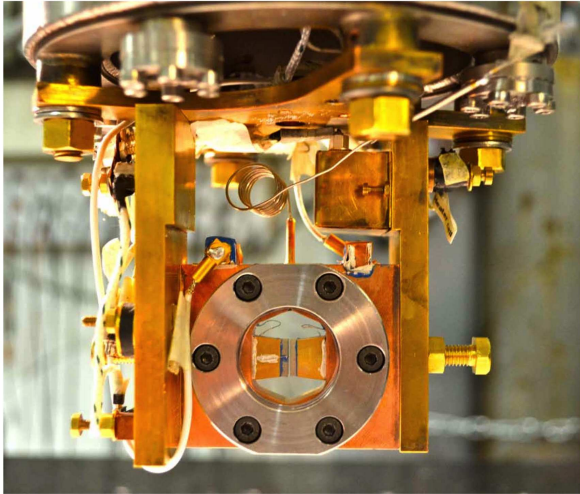

FIG. 1: The second cell used for this experiment is a 5 cm^3 hole in a 15 mm thick Copper plate that is closed with two glass windows sealed with stainless steel clamps and Indium rings. The cell plate is attached to a dilution refrigerator which allows measurements down to 15 mK. ^{4}He crystals are grown inside the 0.7 mm gap between two piezo-electric transducers by injecting liquid through a 0.4 mm capillary on the top (see Figure 2). The two transducers allow applying a vertical shear and measuring the resulting stress across the thin crystal in the gap. A first cell was used for this experiment, where the gap was 1.2 mm thick. The optical access allows determining the crystal orientation (see Figure 3).

bending near their edges. Figure 2 shows the "loading curve", that is the stress measured as crystallization proceeds from the bottom to the top of the transducers. Note that this curve shows no particular singularity at half loading when the liquid-solid interface passes over the two soldering points of grounding leads that are visible on Figure 3. One of these soldering points is on the front and the other on the back so that there is no significant variation in the gap thickness there. Figure 3a shows the shape of a seed during fast growth, which is used to determine the crystal orientation before the crystal is regrown more slowly over the entire cell including the gap between the two transducers (Figure 3b). An ac-voltage (1 mV to 1V at a frequency in the range 1 to 20 000 Hz) is applied to one transducer, which produces a vertical displacement u, consequently a strain $\varepsilon = u/d$ and finally a stress $\sigma = \mu\varepsilon$ on the other transducer (μ is the shear modulus of the He crystal). The displacement u is very small - of order 1 Angstrom per Volt - and it needs to be accurately calibrated in order to obtain an absolute value for μ. The stress generates charges, which are collected as a current whose amplitude and phase are measured with a lock-in amplifier. We also use current pre-amplifiers (femto-lca-20k-200m and femto-lca-200-10g) as was done by Day and Beamish who introduced this method in their original work [2]. We improved their method by calibrating the transducers' response in the following way. We first measured the cross talk between transducers. Although the transducer sides facing each other are grounded, there is a small cross talk between them, which mainly comes from capacitive coupling and needs to be accurately known as a function of frequency. It is independent of pressure and temperature in our working conditions so that we measured it with the cell full of liquid. As explained in the main text, we then used a particular crystal (X3), which was oriented with a [0001] axis tilted by an angle very close to 45° from vertical. For this crystal, the response to a vertical shear depends mainly on the three elastic coefficients c_{11}, c_{13} and c_{33}, with a negligible contribution from c_{44} and c_{66}. The coefficients c_{44} and c_{66} contribute to the shear modulus in all directions except for a shear at 45° from the [0001] axis. We then verified that the measured shear modulus was independent of temperature in our geometry for this particular crys-
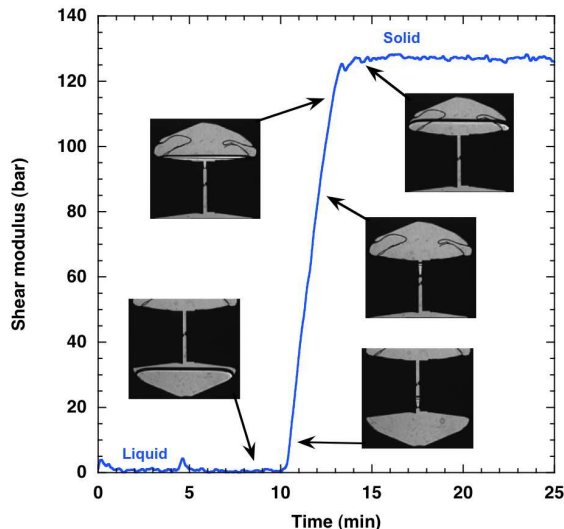
FIG. 2: The loading curve is the shear stress measured in the cell as a function of time during the growth of the crystal in the gap, which takes about 3 minutes in this case. Near the mid height of the transducers, one sees two point contacts for the grounding of the transducer surfaces that face each other. One of these contacts is on the front and the other on the back side of the transducer, so that there is no significant variation in the gap thickness there. Thanks to this design, the loading curve shows a linear variation with height with no singularity at half loading.

tal (see Fig. 3 in the main text). Finally, we used the known values [7, 8] of c_{11}, c_{13} and c_{33} to obtain the piezo-electric coefficient we needed. In the first cell it was d_{15} = 0.88 Angstrom/Volt independently of T up to 1 K and 0.95 in the second cell, about 5 times less than at room temperature. The shear modulus is $\mu = Id/(\omega d_{15}^2 A \sigma)$, where V is the voltage applied to the first transducer, A is the transducers' area (1.2 cm^2 in the first cell and 1 cm^2 in the second one), I is the current generated by the stress on the second transducer. In order to know I, a careful calibration of the gain of our amplifiers needed to be done as a function of frequency. In the end we obtained the absolute amplitude of the real and imaginary part of the response, that is the shear modulus μ and the dissipation $1/Q = tan(\phi)$ where ϕ is the phase delay of the response. For each crystal orientation, we calculated μ as a function of the 5 elastic coefficients (see below), so that we could extract the variation of c_{44}.

SAMPLE PREPARATION

The quality and the purity of samples are very important in this experiment. The crystal quality depends on growth conditions as previously explained by Sasaki *et al.* [3] and by Pantalei *et al.* [4]. The best crystals, called "type 1", are grown relatively slowly (up to 50 μm/s in

this experiment, 0.3 μm/s in the experiment by Rojas *et al.* [5]) at low T, usually around 20 mK, by pressurizing superfluid ^{4}He up to the liquid-solid equilibrium pressure P_{eq} = 25.3 bar. After nucleation on a random site, a crystal seed grows, falls down to the bottom part of the cell and the growth proceeds at constant T and P thanks to the mass injection into the cell through the fill line where helium remains liquid. This fill line is thermally anchored along its path to the cell, so that growth does not warm up the cell even at temperatures less than 20 mK in this experiment. At the equilibrium or during slow growth, the crystal occupies the lower part of the cell with a horizontal surface and some capillary effects where it touches walls, as would a non-wetting liquid in a little glass bottle. This is because the growth dynamics proceeds with negligible dissipation and because the temperature is highly homogeneous so that there are no temperature gradients, only a gravity field [1]. In order to fill the cell with solid as much as possible, one has to place the orifice of the fill line at the highest point in the cell. For this purpose, our cells are tilted. One also has to avoid corners or slits where liquid would be trapped because of capillary effects. Finally, it is also important to avoid the presence of dust particles on walls because they are efficient pinning sites for the liquid-solid interface moving up. If one stays at P_{eq} at the end of the growth, there necessarily remains some liquid in corners or slits, in our case at the junction between the glass windows and the cell body. As a consequence, the ^{3}He impurities may be trapped in this liquid if growth takes place at low T, because their solubility in the liquid is much higher than in the solid [4]. According to our experience, it is also possible to expel all ^{3}He impurities in this adjacent liquid by applying a large ac-stress on the crystal at low T, because the resulting force shakes the dislocation and detaches them from the ^{3}He atoms that are known to travel ballistically through the crystal lattice so that they reach liquid regions in a short time and stay trapped there.

We use a different growth procedure for "type 2" crystals. We grow them again at constant T and P from the superfluid liquid, but at 1.4 K. When the cell is as full of solid as possible, we block the fill line by increasing the pressure outside and we cool down to 1 K at constant volume. Due to the decrease of P_{eq} from 26.1 bar at 1.4 K to 25.3 bar at 1 K, the rest of the liquid in the cell crystallizes but the quality of the final crystal, which occupies the whole cell now, is expected to be damaged by stresses. The advantage of this method is that it produces a crystal in which the ^{3}He concentration is known, equal to the initial concentration in the gas cylinder, and stays at this value during temperature cycles afterwards. Since it is easy to melt or grow crystals by manipulating valves outside the refrigerator, we could melt any "type 1" crystal to a small seed and regrow it as a "type 2" crystal or vice versa.
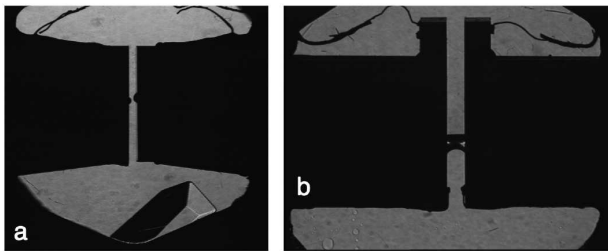
FIG. 3: Two photographs showing the growth shape of a seed crystal on the left (a), and the growth inside the gap on the right (b). The total width of the cell is 20 mm. The growth of the seed is fast enough (1 mm/s) to make facets visible on the left photograph (a) and to allow the determination of the crystal orientation (here crystal X3 with its c axis tilted at 45° from the vertical). The growth inside the gap is shown on the right photograph (b). Here it is our first cell where the gap is slightly larger, 1.2 mm instead of 0.7. The growth inside the gap is slower (50 μm/s). In this first cell, the two transducers were not glued on their entire surface and the electrical contacts were made on the bottom edge of the transducers. Between the two transducers, one can see a straight horizontal line, which is the solid-liquid interface outside the gap, and a convex one below, which shows the capillary depression of the meniscus inside the gap. This depression is a consequence of a 45° contact angle with the transducer walls (for more details on this partial wetting, see [6]).

"Type 3" crystals are polycrystals grown at constant volume from the normal liquid above the superfluid transition. This is known as the "blocked capillary" (BC) method because, when cooling starts, a solid plug forms in the fill line near the "1K pot" of the refrigerator after what the growth proceeds at constant volume and constant mass (but at varying P and T of course). In this experiment, we started cooling down the cell around 3 K with 60 bars everywhere. In the cell, the crystallization started at 2.4 K and finished at 1.7 K with a final pressure P= 30 bar (see "path A" in the phase diagram of ref. [3]). We chose these values to avoid crossing the reappearance of liquid near the hcp-bcc transition of the solid (see [3]). Indeed, recrystallization from the superfluid usually ends up with a few large single crystals while our goal was to obtain isotropic polycrystals with small grains and a strong disorder. The polycrystalline nature of the sample is probably a consequence of multiple nucleations of seeds in a cell that is far from homogeneous in temperature in the absence of superfluid. We found that the crystals grown at the lowest temperature have the largest softening, that is the largest reduction of c_{44} in the soft state. This is probably because their dislocation density Λ is smaller, with a larger free length L between pinning sites (a larger "pinning length"). The precise measurement of Λ and L is in progress in our laboratory.

In this experiment, we reached 80% reduction of c_{44} with the "type 1" crystal X4 . In a previous experiment,

Rojas *et al.* [5] had found an 86% reduction of c_{44}, after assuming that no other elastic constant varied, for another "type 1" crystal which was probably of even better quality for two reasons. First, the growth rate used by Rojas *et al.* was significantly lower (0.3 μm/s) than in this experiment (50 μm/s). Secondly, Rojas' cell had a much more open geometry with no corners and a larger horizontal cross section area, which allowed much more continuous growth without sharp jumps each time the liquid-solid interface detaches from some pinning site.

In their experiment, Ruutu *et al.* [10] obtained small crystals with no screw dislocations according to their measurements of growth rates. Their crystals were grown slowly at 20 mK, but the dislocation density probably depends on the growth speed just after nucleation, which is difficult to monitor. We have not yet succeeded in preparing crystals without any dislocation but it is obviously an exciting challenge because we expect the disappearance of plasticity in that case.

ORIENTATION DEPENDENCE

A little geometry has been necessary for the data analysis. The elastic tensor of an hcp crystal involves 5 independent coefficients c_{ij} with values of i,j from 1 to 6 and writes:

$$\begin{pmatrix} c_{11} & c_{12} & c_{13} & 0 & 0 & 0 \\ c_{12} & c_{11} & c_{13} & 0 & 0 & 0 \\ c_{13} & c_{13} & c_{33} & 0 & 0 & 0 \\ 0 & 0 & 0 & c_{44} & 0 & 0 \\ 0 & 0 & 0 & 0 & c_{44} & 0 \\ 0 & 0 & 0 & 0 & 0 & c_{66} \end{pmatrix}$$

The meaning of these indices from 1 to 6 is respectively xx, yy, zz, yz, xz and xy with the z-axis parallel to [0001], the six-fold symmetry axis - also called "c" - of the hexagonal structure. The coefficient $c_{66} = (c_{11}-c_{12})/2$. The orientation of the x-axis in the plane perpendicular to the c axis is arbitrary since we assume that the dislocations are distributed such that the transverse isotropy of the hcp crystal is preserved. In our experiment, the axis c is tilted with respect to the vertical direction z' of the shear. The crystal orientation is given by the angles θ and ϕ as defined on Figure 4 where the growth shape is compared with a hexagonal prism. Coordinate transformations can be applied to quantities expressed in abbreviated notation using the Bond matrices [14]. Rotations of the coordinate system about its y-axis are applied with:

$$M_y(\eta) = \begin{pmatrix} cos^2\eta & 0 & sin^2\eta & 0 & -sin2\eta & 0 \\ 0 & 1 & 0 & 0 & 0 & 0 \\ sin^2\eta & 0 & cos^2\eta & 0 & sin2\eta & 0 \\ 0 & 0 & 0 & cos\eta & 0 & sin\eta \\ \frac{1}{2}sin2\eta & 0 & -\frac{1}{2}sin2\eta & 0 & cos2\eta & 0 \\ 0 & 0 & 0 & -sin\eta & 0 & cos\eta \end{pmatrix}$$

and rotations about its z-axis are applied with:

$$M_z(\xi) = \begin{pmatrix} cos^2\xi & sin^2\xi & 0 & 0 & 0 & sin2\xi \\ sin^2\xi & cos^2\xi & 0 & 0 & 0 & -sin2\xi \\ 0 & 0 & 1 & 0 & 0 & 0 \\ 0 & 0 & 0 & cos\xi & -sin\xi & 0 \\ 0 & 0 & 0 & sin\xi & cos\xi & 0 \\ -\frac{1}{2}sin2\xi & \frac{1}{2}sin2\xi & 0 & 0 & 0 & cos2\xi \end{pmatrix}$$

The elastic tensor in the transducer coordinate system x'y'z' (Figure 4) is given by:

$$C' = M_z(-\phi)M_y(-\theta)CM_y^T(-\theta)M_z^T(-\phi)$$

where X^T is the transpose of matrix X.

The shear modulus that relates the shear strain we apply to the component of the shear stress that we measure is given by:

$$\mu = c'_{44} = \frac{1}{4}(c_{11} - 2c_{13} + c_{33})sin^2 2\theta sin^2\phi +$$
$$c_{44}(cos^2\theta cos^2\phi + cos^2 2\theta sin^2\phi) + c_{66}cos^2\phi sin^2\theta$$

We used the above equation to calculate the shear modulus μ as a function of the coefficients cij for all our crystals. For example we obtained:

$\mu = 0.0001(c_{11} - 2c_{13} + c_{33}) + 0.933c_{44} + 0.067c_{66}$ for X2
($\theta = 89.5°$ and $\phi = 85°$)

$\mu = 0.25(c_{11} - 2c_{13} + c_{33}) + 0.004c_{44} + 0.004c_{66}$ for X3
($\theta = 45°$ and $\phi = 85°$)

$\mu = 0.0001(c_{11} - 2c_{13} + c_{33}) + 0.25c_{44} + 0.56c_{66}$ for X5
($\theta = 60°$ and $\phi = 30°$)

$\mu = 0.008(c_{11} - 2c_{13} + c_{33}) + 0.97c_{44}$ for X21
($\theta = 5°$ and $\phi = 90°$)

The values of all c_{ij} have been obtained from ultrasound velocity measurements at 10 MHz by Crepeau *et al.* at 1.32K [7] and by Greywall at 1.2K [8] $c_{11} = 405$ bar, $c_{12} = 213$ bar, $c_{13} = 105$ bar, $c_{33} = 554$ bar, $c_{44} = 124$ bar, and $c_{66} = 96$ bar. At such high temperatures, the damping of dislocation motion by thermal phonons being proportional to the frequency and to T^3, [12] dislocations cannot move at 10 MHz. As a consequence, their values correspond to the true elasticity of the lattice, without any contribution from plasticity. We have verified that, at low temperature in the presence of ^{3}He impurities, the shear modulus of our ^{4}He crystals is the
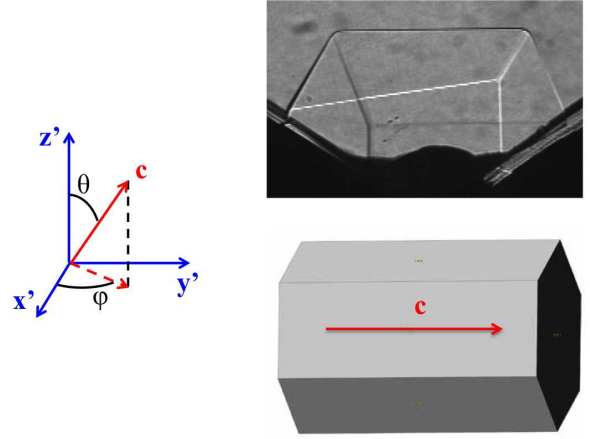

FIG. 4: The crystal orientation. The orientation of the [0001] axis "c" is defined by two angles θ and ϕ. The axis z' is vertical, parallel to the transducer plane surfaces. The axis x' is perpendicular to the windows, and the axis y' is perpendicular to the transducer surfaces. The values of θ and ϕ are obtained by matching the growth shape with a hexagonal prism. In this particular case (crystal X2), the c axis is very close to horizontal. On the photograph, one sees that the crystal touches the front window so that two white lines correspond to intersections of the crystal with this front window. Only the free edges of the crystal are used to determine the orientation.

same as measured by Crepeau *et al.* [7] and by Greywall [8]. The only correction to be made for polycrystals grown at high pressure is the pressure dependence analysed by H.J. Maris [9].

The resolved stress σ_r is the quantity which determines the force acting on dislocations. We determined it as follows. The strain in the transducer coordinate system (Figure 4) is given by:

$$E' = \begin{pmatrix} 0 & 0 & 0 & \varepsilon & 0 & 0 \end{pmatrix}^T$$

In the crystal frame this becomes:

$$E = M_y(\theta)M_z(\phi)E'$$

The stress in the crystal frame is then :

$$\Sigma = CE$$

The magnitude of the resultant of the shear stresses acting in the basal plane $(\Sigma_4^2 + \Sigma_5^2)^{1/2}$ is independent of rotations of the crystal about its c-axis. If we assume that the three $\langle 11\bar{2}0 \rangle$ Burgers vectors are uniformly populated then we can choose the convenient orientation with one set of Burgers vectors along the stress resultant and the other two at 60° to it. Then the average resolved stress will be:

$$\sigma_r = \frac{c_{44}\varepsilon\sqrt{cos^2\theta cos^2\phi + cos^2 2\theta sin^2\phi}}{\sqrt{3}}$$

TEMPERATURE CYCLES AND ANNEALING OF SAMPLES

Most of the data that are analysed in this article have been obtained by cooling samples slowly (12 hours) from 1 K down to 15 mK. The first reason for proceeding this way is that we confirmed that some disorder induced by mechanical perturbations at low T is annealed when warming above 0.5 K, as was previously noticed by Day *et al.* [12]. Each temperature cycle took 6 hours for warming up to 1 K and 12 hours for cooling down to 15 mK, that is about one day. We used the same procedure for all crystals in order to include a recording during the night when perturbations from the environment were as small as possible (remember that we measure stresses down to 1 nanobar; He crystals are extremely sensitive to vibrations). We then transferred liquid Nitrogen every morning when the crystal was cold. Every three days, a liquid helium transfer was also necessary to keep the refrigerator working. All these transfers produce mechanical vibrations that shake dislocations. After any large mechanical perturbation at low temperature, we observe some hardening of crystals, which we believe is due to creation of jogs on the dislocations. After annealing up to 1 K we found reproducible results as if jogs had been eliminated thanks to the diffusion of thermally activated vacancies.

COMPARISON WITH A CLASSICAL CRYSTAL

In order to compare the plasticity in helium crystals and in classical crystals, let us consider the historical measurements by Tinder and Washburn[15] on Copper. Qualitatively, the plasticity is the same phenomenon: it is due to the motion of dislocations and it is sensitive to the concentration of impurities. But quantitatively, there are striking differences. Tinder and Washburn found a threshold stress of about 2 g/mm^2 = 2 10^4 Pa beyond which a plastic strain appears in addition to the usual elastic response. This threshold is somewhat smaller than in other classical crystals, probably because of the careful growth and manipulation of these very pure samples. Still, it is larger by five orders of magnitude than in our case. In Copper, the applied stress is 0.4 10^{-6} times the shear modulus μ_{Cu} = 50 GPa. For helium crystals, we find a linear response (no threshold) down to 1 nanobar = 10^{-4} Pa, which is 10^{-11} times the elastic shear modulus μ_{He} = 12 MPa. Furthermore, Tinder and Washburn find a plastic strain that is 40 times *smaller* than the elastic strain so that the effective shear modulus is not significantly changed. In Helium, the plastic strain due to the dislocation motion is 4 times *larger* than the elastic strain, leading to an effective shear modulus that is reduced by 80%. In other words, the plastic response is 2 orders of magnitude larger for stresses 5 orders of magnitude smaller than in Copper. In Copper, the plastic response is highly non-linear and the response time of order minutes at room temperature (300 K). In Helium at 0.1 K, the plasticity is linear so that it results in an effective reduction of the shear modulus, which we have found independent of frequency up to 16 kHz. We have been able to study oriented single crystals and we have found evidence that the gliding plane of dislocations is the basal plane, so that the plasticity is anisotropic. Tinder and Washburn studied polycrystalline samples where they could not measure any orientation dependence of the plasticity.

[1] A. Berghezan, A. Fourdeux, and S. Amelinckx, Acta Metall. **9**, 464-490 (1961).
[2] J. Day and J. Beamish, Nature **450**, 853 (2007).
[3] S. Sasaki, F. Caupin, and S. Balibar, J. Low Temp. Phys. **153**, 43 (2008).
[4] C. Pantalei et al. J. Low Temp. Phys. **159**, 452 (2010).
[5] X. Rojas, A. Haziot, V. Bapst, S. Balibar, and H.J. Maris, Phys. Rev. Lett. **105**, 145302 (2010).
[6] S. Balibar, A.Y. Parshin, and H. Alles, Rev. Mod. Phys. **77**, 317-374 (2005).
[7] R.H. Crepeau et al. Phys. Rev. A **3**, 1162 (1971).
[8] D.S. Greywall, Phys. Rev. B **16**, 5127 (1977).
[9] H.J. Maris and S. Balibar, J. Low Temp. Phys. **160**, 5 (2010).
[10] J.P. Ruutu et al. Phys. Rev. Lett. **76**, 4187 (1996).
[11] PZT ceramics from Boston Piezo-Optics Inc., USA.
[12] J. Day, O. Syshchenko, and J. Beamish, Phys. Rev. **B 79**, 214524 (2009).
[13] A. V. Granato and K. Lcke, J. Appl. Phys. **27**, 583 (1956).
[14] B. A. Auld, Acoustic Fields and Waves in Solids, Vol. 1, (Krieger, Malabar, 1990).
[15] R.F. Tinder and J. Washburn, Acta Met. 12, 129 (1964).